PHILOSOPHICAL TRANSACTIONS OF THE ROYAL SOCIETY A MATHEMATICAL, PHYSICAL & ENGINEERING SCIENCES

Dynamo simulation and palaeosecular variation models

Masaru Kono, Ataru Sakuraba and Mizuho Ishida

Phil. Trans. R. Soc. Lond. A 2000 **358**, 1123-1139
doi: 10.1098/rsta.2000.0577

THE ROYAL SOCIETY

Dynamo simulation and palaeosecular variation models

By Masaru Kono[1], Ataru Sakuraba[2] and Mizuho Ishida[3]

[1]*Institute for Study of the Earth's Interior, Okayama University, Yamada 827, Misasa, Tottori-ken 682-0193, Japan*
[2]*Department of Earth and Planetary Physics, University of Tokyo, Hongo 7-3-1, Bunkyo-ku, Tokyo 113-0033, Japan*
[3]*National Research Institute for Earth Science and Disaster Prevention, Tennodai 3-1, Tsukuba, Ibaragi-ken 305-0006, Japan*

In this paper we examine the simulation results of a fully nonlinear, three-dimensional dynamo and obtain inferences useful in the study of present and past geomagnetic field. This approach has importance because of the limitation in the available data of the real magnetic field: the present field is known with a high accuracy, but the time covered is only a small fraction of the time constant inherent to the geodynamo, while palaeomagnetic data provide data for a long time-span, but they are of poor quality and are distributed quite irregularly both in space and time. Thus, we compare what we see from the external field of the dynamo model with the features established or conjectured for the present or palaeomagnetic fields. We show that some of the statistical properties of the magnetic field generated by dynamo models compare well with those of the real magnetic field: dominance of the axial dipole, similar power in each degree of the harmonic at the core surface, nearly normal distribution of Gauss coefficients, and the lack of correlation among their variations. Differences were observed in other features, such as drift in the azimuthal direction and concentration of magnetic flux in small patches at the core surface. They can be attributed to either the shortness of the observational period, or to the difference in the resolution of the models, which suppresses small-scale features far below the level of the observation.

Keywords: dynamo simulation; palaeosecular variation; statistical properties

1. Introduction

Direct observation from the time of Gauss has shown various features of the geomagnetic field that must reflect some intrinsic properties of the Earth's dynamo. Since the 1980s, availability of vector data from satellites (e.g. Langel *et al*. 1980), the use of the modern inversion method, and incorporation of pre-observatory data (Gubbins & Bloxham 1985; Bloxham & Jackson 1992) has increased the accuracy of and extended the time-intervals covered by the models of the recent field. The present and recent data are associated with small errors, and descriptions of the field based on these data are quite precise as well as detailed. However, these data have severe limitations in that the time-span covered is only a fraction of the natural time constant of the geodynamo.

On the other hand, palaeomagnetic observations provide data covering millions of years, and reveal phenomena which were not seen by the direct observations because they have long time constants (e.g. palaeosecular variation) or are rare events that have not occurred in recent times (e.g. reversals and excursions). The quality of palaeomagnetic data, however, is quite poor compared with the recent data. Moreover, most of the data are poorly distributed on the globe and inaccurate in age. For these reasons, we have to use statistical treatments in most of the field analyses based on palaeomagnetic data in trying to see global features of the magnetic field.

Recently, simulation of the fully three-dimensional, nonlinear dynamos became possible (Kageyama & Sato 1995; Glatzmaier & Roberts 1995*a*, *b*). As behaviours of the magnetic field can be reconstructed in good detail from the results of dynamo simulation, it is interesting to examine them to see if the dynamo models show behaviour similar to that observed for the geomagnetic field. It may also be possible to judge the viability of some of the commonly employed assumptions about the nature of the geomagnetic field through the analysis of numerical results. This paper intends to examine the numerical results of Sakuraba & Kono (1999) with these objectives.

At this point it is instructive to consider the rationale and the limitation of such a comparison. The dynamos are characterized by a number of non-dimensional parameters. Because of the difficulty of using parameters relevant to the real Earth, the dynamo models reported thus far cannot be said to be really representative of the conditions prevailing in the Earth's core. Although recent dynamo models treat fully nonlinear and three-dimensional situations, they are still far from the real state of the Earth. Also, the numerical results are not yet abundant enough, so that our results, for example, cannot be taken as representative examples. Even with these limitations, it can be said that these simulation results are at least physically well founded, and comparison with observations may point out some features that are not very sensitive to the choice of particular values of parameters or boundary conditions. Our intention is, therefore, to try to pick up more or less general properties of a certain type of dynamos, as represented by the Earth.

2. The dynamo model

Sakuraba & Kono (1999) reported two simulation results of a magnetohydrodynamic dynamo in a rapidly rotating sphere and spherical shell under the Boussinesq approximation. In the present study, we refer only to the results for the spherical shell, as they are more appropriate for the Earth. In Sakuraba & Kono (1999), the Navier–Stokes equation for the velocity $\boldsymbol{u}$, the thermal conduction equation for the temperature T, and the induction equation for the magnetic field $\boldsymbol{B}$ were simultaneously solved. Besides these equations, both $\boldsymbol{u}$ and $\boldsymbol{B}$ satisfy the divergence-free condition, and the density of fluid is treated as constant except for the small change proportional to the temperature fluctuations.

The convection and, consequently, the magnetic field were energized by buoyancy force due to the heating of the fluid by a heat source distributed homogeneously both in the outer and the inner core. The inner core had a radius equal to $0.4R_{\mathrm{C}}$, where R_{C} is the radius of the outer core, and had the same physical properties as the fluid outer core, except that it was treated as a rigid body (the same thermal and magnetic diffusivities κ and η, but not the kinematic viscosity ν). The inner core

Table 1. *Non-dimensional parameters used in the simulation*

(R_C is the radius of the core. Ω is the rotation rate of the mantle. α is the thermal expansivity. β is the reference temperature gradient at the CMB. g_0 is the gravitational acceleration at the CMB. V is the typical value of the velocity of the fluid. ν, κ and η are the kinematic, thermal, and magnetic diffusivities, respectively.)

name	symbol	definition	model value	value for Earth
Rayleigh number	Ra	$\alpha\beta g_0 R_C^4/\kappa\nu$	1×10^7	6×10^{30}
Ekman number	E	$\nu/2\Omega R_C^2$	3.16×10^{-5}	10^{-15}
Rossby number	Ro	$V/\Omega R_C$	4×10^{-3}	3×10^{-7}
Prandtl number	Pr	ν/κ	1	0.1
magnetic Prandtl number	Pm	ν/η	20	10^{-6}

can rotate freely under the viscous and electromagnetic torques applied by the outer core. The core–mantle boundary (CMB) was assumed to be a rigid boundary for the fluid motion, and the magnetic field was continued to the source-free field outside the CMB. The non-dimensional parameters used in this simulation are summarized in table 1 and compared with values thought to be relevant to the core of the Earth (Gubbins & Roberts 1987).

The equations were solved in spherical polar coordinates (r, θ, ϕ) using a spectral transform method similar to the one described by Glatzmaier (1984). The vectors $\boldsymbol{u}$ and $\boldsymbol{B}$ were decomposed into toroidal and poloidal scalars by virtue of the divergence-free condition, and all the scalar variables were expanded into spherical harmonics Y_ℓ^m in θ and ϕ, and into Chebyshev polynomials T_n in r. The truncation level of spherical harmonics was 43, while that for Chebyshev polynomials was 32 for the outer core and 10 for the inner core.

The linear part of the equation was solved implicitly by the Crank–Nicholson method. For time stepping other terms were treated by the Adams–Bashforth scheme. For the calculation of nonlinear terms such as $\nabla \times (\boldsymbol{u} \times \boldsymbol{B})$, the coefficients in spectral space were transformed into physical space, multiplied there, and then transformed back to spectral space (pseudo-spectrum method). The time step for integration was taken to be about 4×10^{-6} in non-dimensional units. The results were recorded at intervals of 0.0025 time units, in the form of Legendre–Fourier–Chebyshev coefficients.

3. Characteristics of the magnetic field

Below we compare various features of the numerical simulation results with those of the present field or those derived or assumed from the analyses of the present or palaeomagnetic data. For the numerical data, we use the results of Sakuraba & Kono (1999) for the time-interval between 3 and 6 non-dimensional units. The present field model used for comparison was taken from Bloxham & Jackson (1992), which has coefficients up to degree 14 and covers the interval 1690–1990.

The unit of non-dimensional time in Sakuraba & Kono (1999) was R_C^2/η (magnetic diffusion time), but in this paper R_C^2/ν is used instead. As the magnetic decay time of the core may be equated to about 1.5–2×10^5 years, the non-dimensional time for this paper can be obtained by dividing this value by the magnetic Prandtl number

(20); i.e. about 8000–10 000 years. In this paper, we treat 0.1 non-dimensional time-intervals as one thousand years for the sake of simplicity. Thus, the analysed interval corresponds to about 30 000 years.

In the following, the 'surface' field for the dynamo model was calculated with $r = 1.828$, which is the same as the ratio of the radii of the core and that of the Earth (R_E/R_C). To express the magnetic field outside the core, we use a representation that is familiar in geomagnetism: Gauss coefficients g_ℓ^m and h_ℓ^m defined using Schmidt normalized Legendre functions (Langel 1987).

(*a*) *Field morphology*

Figures 1 and 2 compare examples of the distribution of the radial component of the magnetic field for the present (Bloxham & Jackson 1992) and for the dynamo model. It should be remembered that the time-spans represented by the two figures are quite different: 300 years compared with about 6000 years. First of all, both fields are dominated by the dipole. Although the magnetic Equator shows strong undulation, and there are a number of flux patches with the magnetic field of the opposite polarity (the areas surrounded by null flux curves shown by thick dotted lines) in both hemispheres, it can be seen that one hemisphere is dominated by one polarity, and the other hemisphere by the other polarity. As will be shown later, the axial dipole term is by far the largest in the dynamo model, which agrees well with the characteristics of the present field.

Apart from that, the dynamo model shows much more small-scale features than the present field model. This is a natural consequence of the difference in the truncation levels (43 and 14 in harmonic degrees and orders). The present core field model is a result of the downward continuation of the observed surface field, and short wavelength features are intentionally damped to avoid amplification at depth of spurious features due to noise or crustal sources. On the other hand, we know 'exactly' what occurs in the dynamo model at least to the truncation level, and the field at the CMB can be calculated to the full range of harmonics used in the numerical simulation.

More interestingly, we see in both figures a number of places where magnetic flux is strongly concentrated. Such concentrations are found both at relatively high latitudes (*ca.* 50° N or S) and near the Equator (figures 1 and 2). The low-latitude flux concentration occurs because of the strong dynamo generation mechanism in these areas (Sakuraba & Kono 1999). The strong velocity shear below the CMB is responsible for the generation of concentrated toroidal flux near there (ω-effect), and the helical motion induced by the Coriolis force feeds back from the toroidal to the poloidal field (α-effect). It is interesting that similar (although less concentrated) flux patches can be found in the present field near the magnetic Equator (especially in figure 1*c*).

The flux concentrations at high latitudes are related to the form of convection rolls inside the spherical shell. When the magnetic field is absent or weak, several pairs of clockwise and counterclockwise rotating rolls are formed outside the tangent cylinder, which is an imaginary cylinder touching the inner core at its equator (Busse 1975). As the magnetic field grows, this regular structure is modified, but some pairs of convection rolls still remain (Sakuraba & Kono 1999).

The magnetic flux is trapped in the cyclonic convection rolls circulating counter-clockwise as seen from the north at the outer boundary (CMB). This is because

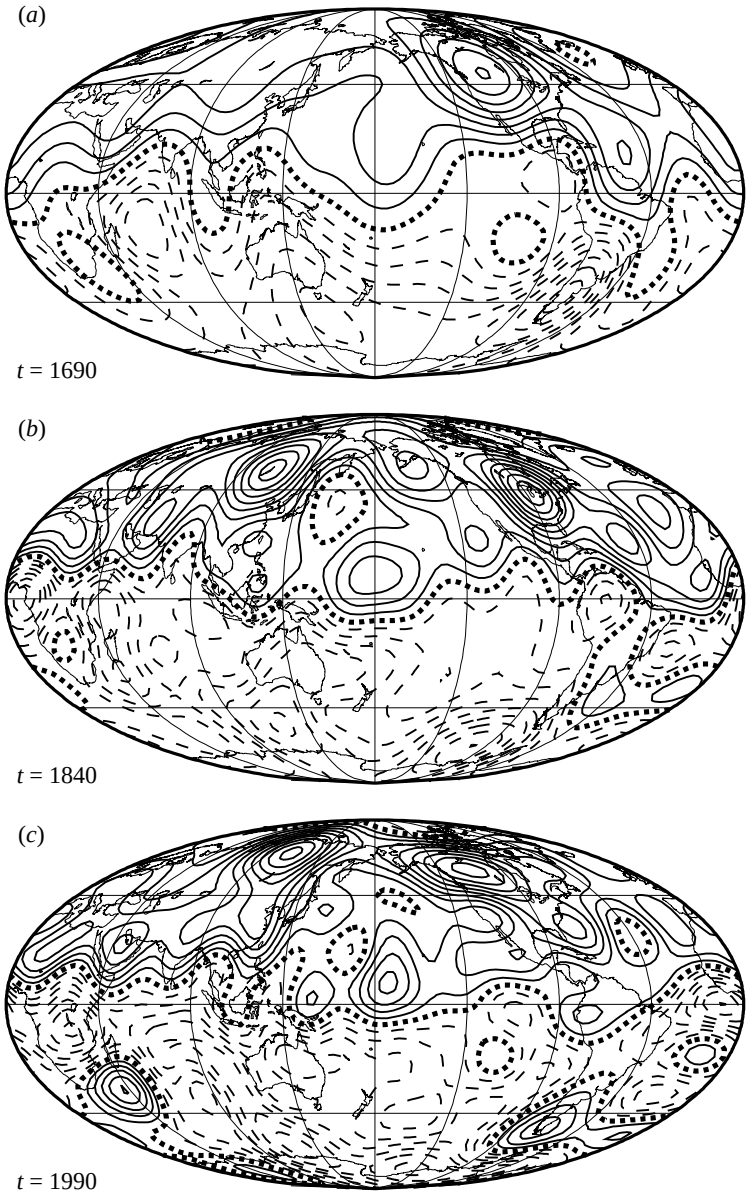

Figure 1. Radial component of the Earth's magnetic field at the core–mantle boundary (CMB) in the last 300 years (Bloxham & Jackson 1992). Continuous and dashed lines indicate that the field is inward or outward at the CMB, respectively. Thick dotted lines indicate the null flux curves. The contour interval is 100 μT.

of the Ekman suction (pumping), which generates inward flow within the Ekman boundary layer at the CMB (Kageyama & Sato 1995; Sakuraba & Kono 1999). In the anticyclones circulating clockwise, the situation is reversed and outward flow is induced by the Ekman pumping. Thus, the magnetic fluxes are 'expelled' from anticyclones and 'sweeped' in the cyclones just below the CMB.

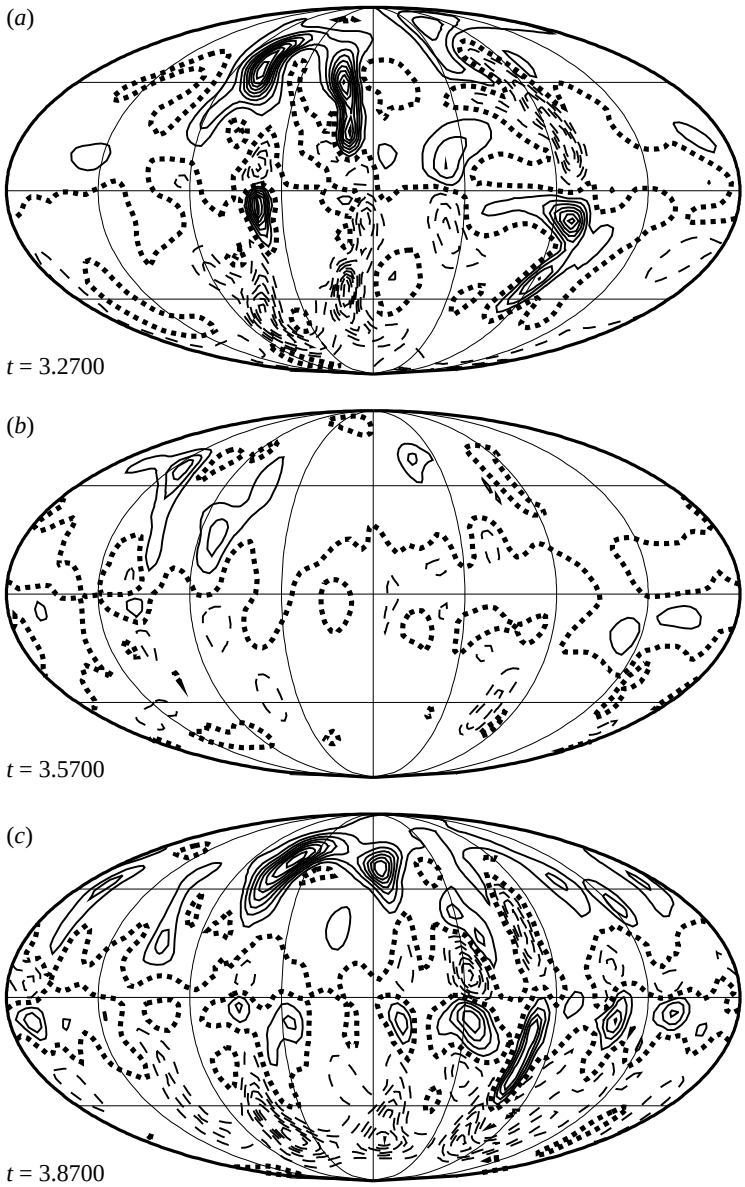

Figure 2. Radial component of the magnetic field at the core–mantle boundary produced by numerical simulation. Continuous and broken lines indicate that the field is outward or inward at the CMB (note the reversed definition with respect to figure 1). Thick dotted lines indicate the null flux curves. Contour interval is 25 non-dimensional units.

When the magnetic field is not strong, there were about seven pairs of cyclonic and anticyclonic convection rolls in our model, and the flow field was nearly periodic in the azimuthal direction. When the field became strong enough, the regularity in the convection was destroyed and the number of rolls was diminished (Sakuraba & Kono 1999). In our simulation, a strong concentration of flux was observed at 2–4 places

in the high latitudes of a hemisphere most of the time (figure 2*a*, *c*). The spacing between these flux concentrations is similar to the distance between the convection rolls when they were more-or-less regularly spaced while the magnetic field was small enough. Sometimes, these features were almost absent, and, consequently, the dipole field was very weak (figure 2*b*). Even in the latter case, the dipole field was still larger than the non-dipole field. We will come back to this point later.

(*b*) *Drift in the azimuthal direction*

One of the best-known properties of the present field is the westward drift, which means that parts of, or the whole of, the non-dipole magnetic field pattern move westwards with a typical velocity of 0.1–0.4 deg yr^{-1} (Bullard *et al*. 1950). Yukutake (1967) showed that some features, such as extrema of inclination or declination at mid-latitudes of the Northern Hemisphere, can be traced back in time for about a thousand years using archaeomagnetic data, and the migration speed was estimated to be 0.3–0.5 deg yr^{-1}.

However, the westward drift is not considered to be a universal property of the geomagnetic field. Yukutake & Tachinaka (1968) showed that some anomalies on the globe are indeed drifting, while others seem to have stayed at about the same place during the whole period of observation. Palaeomagnetic data suggest that the field may sometimes be drifting westwards, but may also be drifting eastwards at other times. In the Bloxham–Jackson field (figure 1), a big negative anomaly in the south Indian Ocean in 1690 seems to move to the east coast of South America in 1990, while positive anomalies in North America and in Siberia seem to stay at about the same longitude. Such 'standing' anomalies were identified earlier (Yukutake & Tachinaka 1968; Bloxham & Gubbins 1995).

A good way of examining the drift in the azimuthal direction is to make longitude–time diagrams of a magnetic field element. Figure 3 illustrates the time change of the vertical component at 40° N on the CMB as given by the dynamo model. There are some features moving to the west, but there are also others moving to the east. Typical drift velocity seems to be about 120° per 0.1 unit time. This corresponds to 0.12 deg yr^{-1} in dimensional units. The westward or eastward drift does not continue to encircle the whole globe. It seems that the areas with concentrated magnetic flux have a life time of less than 0.1 time units, or about 1000 years.

Seen at the surface, the azimuthal movement is quite different from what we saw at the CMB. Figure 4 is the longitude–time plot at the surface for the same time-interval as shown in figure 3. We do not see any trace of the drift of small-scale features observed at the CMB. Instead, a broad trend of drift may be seen, for instance, between 4.4 and 4.8 near 225° longitude. Comparing with figure 3, we see that this corresponds to the slow shift of the broad region of small magnetic activities westwards at the CMB.

The small-scale features at the CMB, however strong, cannot be seen at the surface, as the amplitude of the signal of degree l is reduced to $(R_C/R_E)^{l+2}$ of that at the CMB. If we assume that the degree of a particular feature is about 30, the reduction amounts to a factor of 10^{-8}. This warns us that the surface features such as the westward drift may be difficult to correlate to the activities occurring near the CMB or within the core.

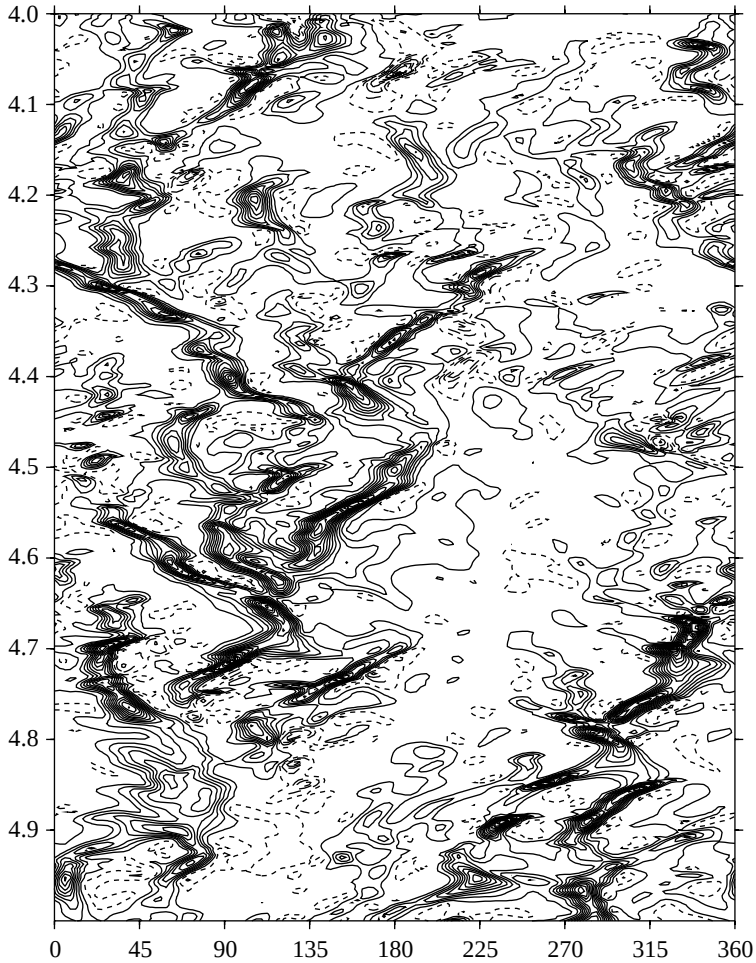

Figure 3. Latitude–time diagram for the dynamo simulation results. Shown in this figure is the radial component at the CMB. The contour interval is 50 non-dimensional units.

(*c*) *Power spectrum*

Langel & Estes (1982) showed that the power of the magnetic field contained in the harmonics of degree l,

$$R_l(r) = (l+1)\left(\frac{R_\mathrm{E}}{r}\right)^{2l+2} \sum_{m=0}^{l} [(g_\ell^m)^2 + (h_\ell^m)^2], \tag{3.1}$$

shows a marked exponential decrease with l at the surface of the Earth ($r = R_\mathrm{E}$), but are nearly constant if calculated at the CMB ($r = R_\mathrm{C}$). The dipole term ($l = 1$) was clearly larger than the trend shown by harmonics of $1 < l < 13$. This behaviour of the so-called Lowes–Mauersberger spectrum (Lowes 1974) is usually taken to indicate that the region of the magnetic field generation for $1 < l < 13$ is within the core. Constable & Parker (1988) used this property to obtain the Giant Gaussian Model for the palaeosecular variation in the last 5 Myr. A similar approach was taken by

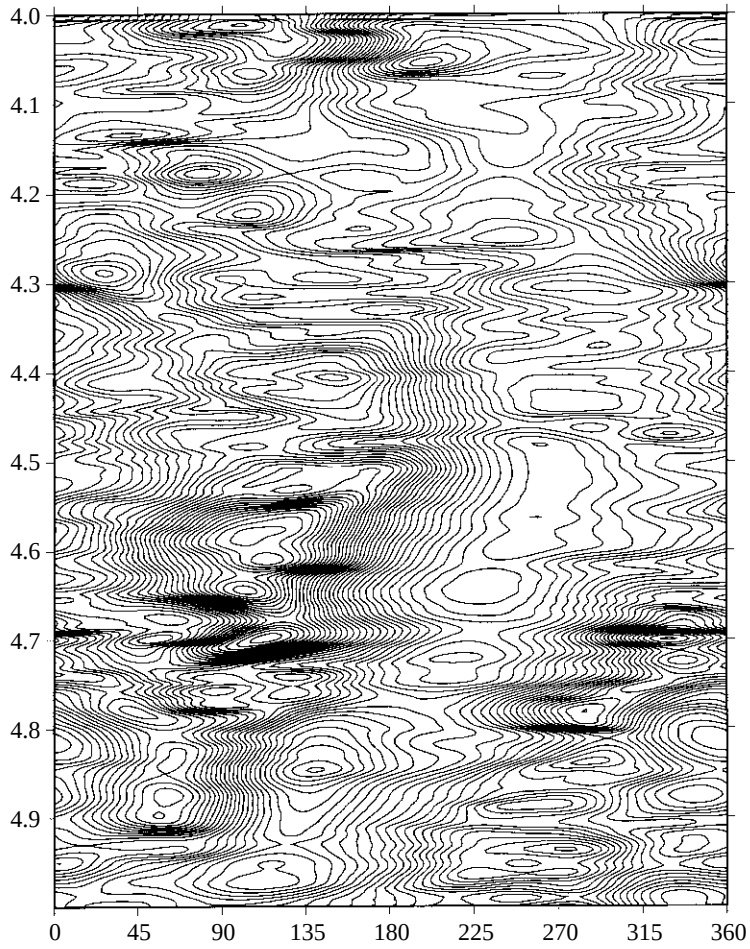

Figure 4. Same as figure 3 but the radial component at the surface is shown in this latitude–time diagram. The contour interval is 1 non-dimensional unit.

Kono & Tanaka (1995), who defined the homogeneous background model (HBM). In these models, the axial dipole term (g_1^0) has a mean different from zero, but most of the other terms are assumed to behave like a normal variate with zero mean and a variance that is constant for the same degree l.

Figure 5 compares the power in each degree (3.1) of the present field and the dynamo field at the surface as well as at the CMB. The trend is impressively similar between the two. On closer examination, it becomes clear that the dynamo results give more 'white' spectrum than the present field. At the CMB, the present field still shows some decrease with increasing degrees (the rapid decrease for $l > 12$ is irrelevant, since it is caused by the regularization scheme imposed in the inversion), while it is nearly flat from $l = 2$ to $l = 14$ in the dynamo model. In both cases, the power of the dipole term is somewhat higher than the trend defined by the non-dipole terms to about $l = 14$. Figure 5*b* shows that the power in the dynamo model at the CMB trails off smoothly and slowly for degrees larger than 20. This

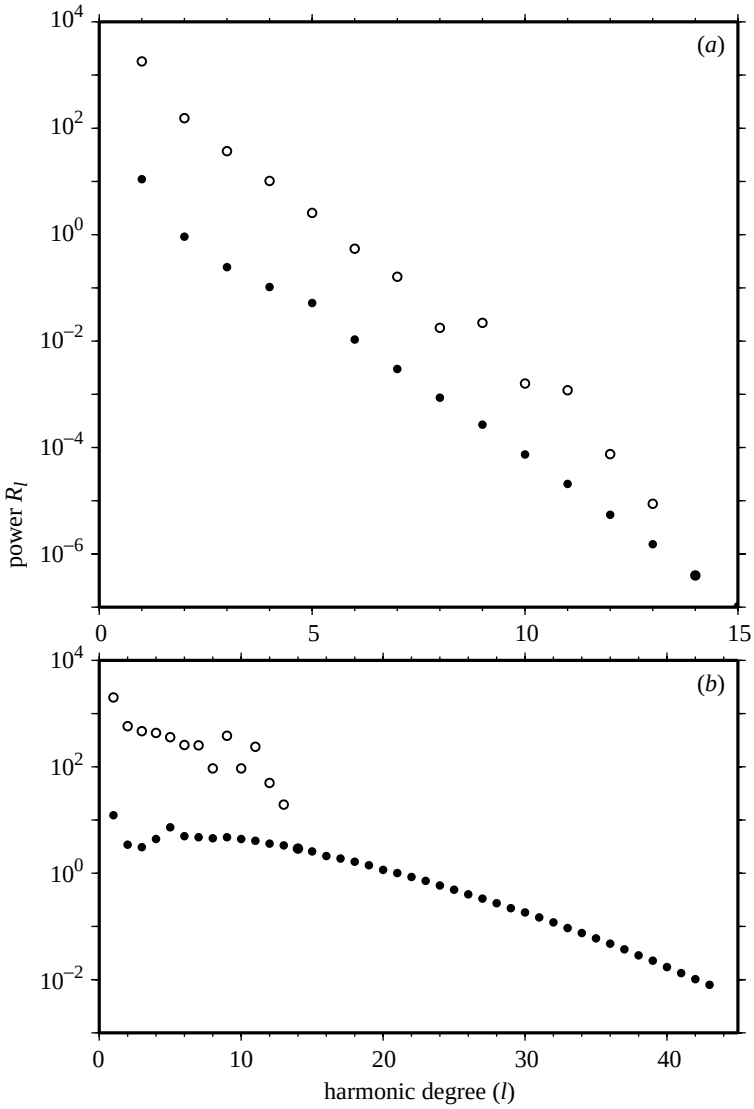

Figure 5. Lowes–Mauersberger spectra at the surface (a) or at the CMB (b) for the present field (open circles) and for the dynamo field (closed circles). The present field is due to Bloxham & Jackson (1992), and the dynamo field shows the mean for the time-interval 3.0–6.0. The unit of power is μT^2 for the present and non-dimensional units for the dynamo model.

is reasonable since the dynamo calculation employed a hyperdiffusivity in the form of $(\nu, \kappa, \eta) = [1 + (l/20)^3](\nu_0, \kappa_0, \eta_0)$, which effectively damps the power at degrees larger than 20 (Sakuraba & Kono 1999).

Glatzmaier & Roberts (1995*b*) showed for their dynamo model a similar diagram for the power at the surface. Besides the comparison in time of well-established polarity, they also showed the spectrum when the field was reversing its polarity. In the latter case, the powers for non-dipole terms of $l > 3$ stayed about the same as that before the reversal started, but the dipole power was markedly reduced.

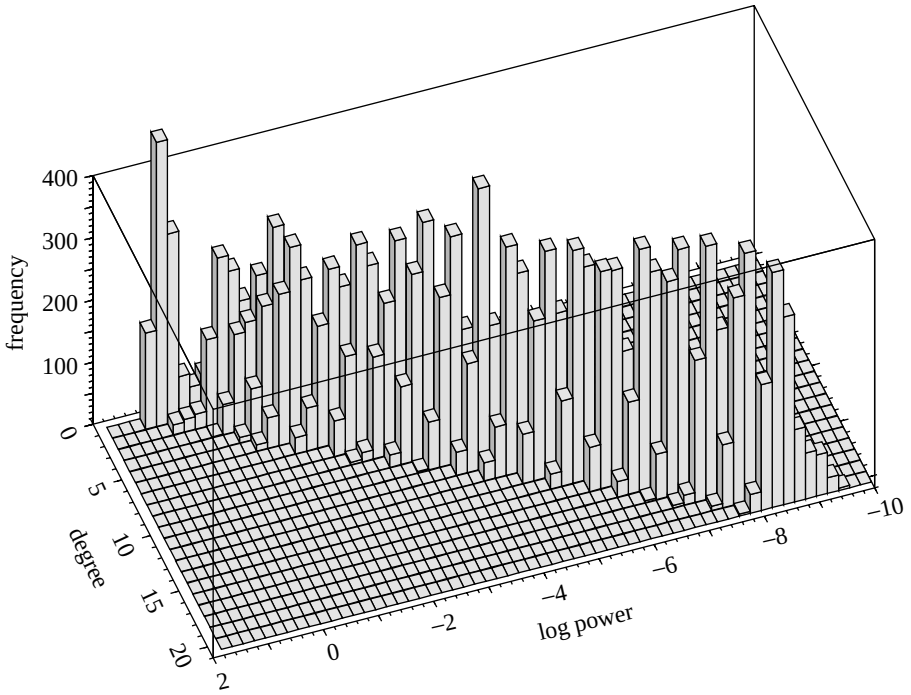

Figure 6. Distributions of powers of the surface magnetic field for each degree (equation (3.1)) derived from dynamo model for the same interval as in figure 5.

Figure 6 shows the distribution of powers of individual degree at the surface. This diagram is constructed by counting the instantaneous values at about 1200 steps. Apparently, a lognormal distribution of the power for each degree and exponential decrease as seen for the means (figure 5) is repeated here.

(*d*) *Distribution of Gauss coefficients*

Constable & Parker (1988) and Kono & Tanaka (1995) derived secular variation models based on the assumption that Gauss coefficients in a sufficiently long time-interval behave as random variates mostly of zero means, except, of course, the axial dipole, which has a definite mean. In the case of Constable & Parker (1988), g_2^0 is also assumed to have a mean different from zero.

Figure 7 shows the distribution functions for Gauss coefficients up to degree 3. Excluding g_1^0 (but including g_2^0), the zero mean assumption seems to be adequate for the coefficients. The shapes of the distributions are not exactly normal, but they have single well-defined modes and trail off to both sides. Thus, it also seems reasonable to assume that they follow a zero mean (except g_1^0) normal distribution.

One thing to be noted from this figure is the large dispersion of (2,1) terms, which coincides with the characteristics of palaeosecular variation in the last 5 Myr (e.g. Kono & Tanaka 1995; Gubbins & Kelly 1995). The range of distribution for g_2^1 and h_2^1 is about three times larger than that for other degree-2 terms (figure 7). A dominantly big part of the power of the degree-2 harmonics are borne by (2,1) terms. The boundary conditions in the dynamo model are homogeneous at the CMB, so this

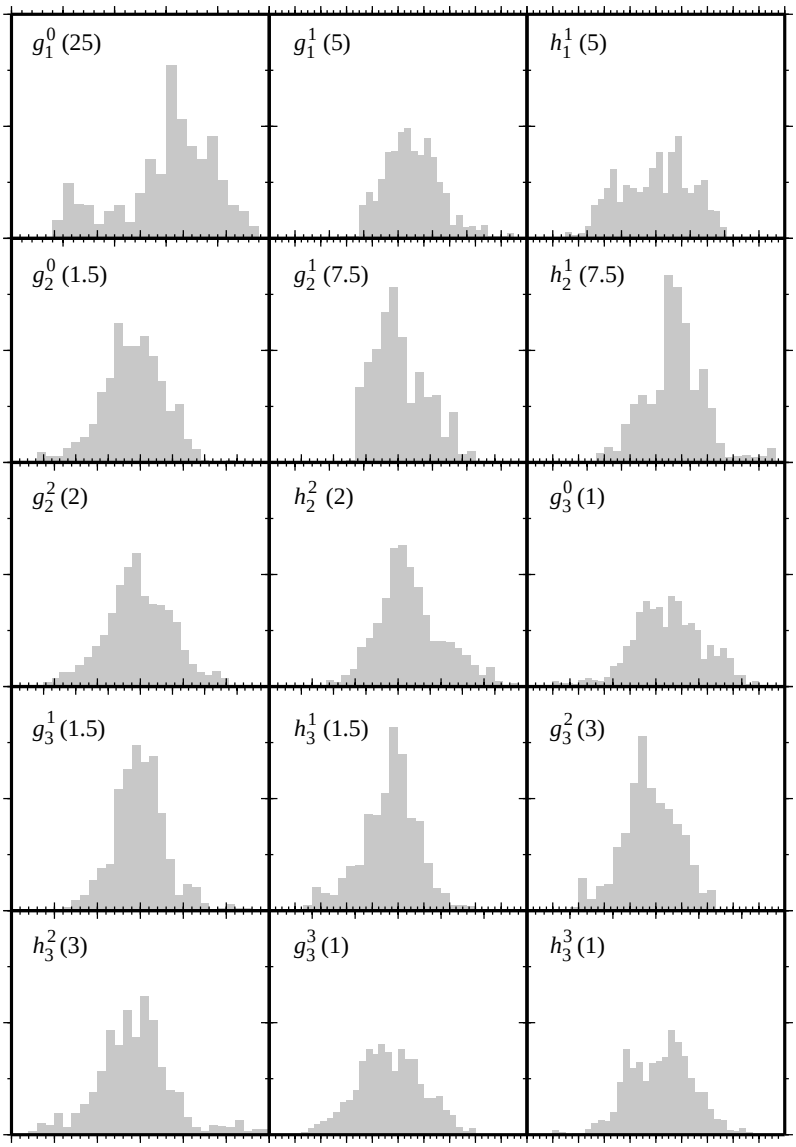

Figure 7. Distribution of the Gauss coefficients obtained from dynamo simulation. About 1300 values in the time-interval 3–6.2 is used. The maximum value of each abscissa is indicated by numbers in the parentheses. The minimum of the abscissa is the negative of the maximum value, except for g_1^0 for which it is 0. The ordinate shows the relative abundance.

bias may be either because the sampling period is too short to express the true nature of the ensemble, or because some interactions in the dynamo mechanism favour these harmonics. The former possibility seems to be unlikely, since the distribution is essentially unchanged if we used a subset of data obtained by subdividing the time-interval. It is, thus, a possibility that generation of large (2,1) harmonics is one property of the Earth-type dynamo.

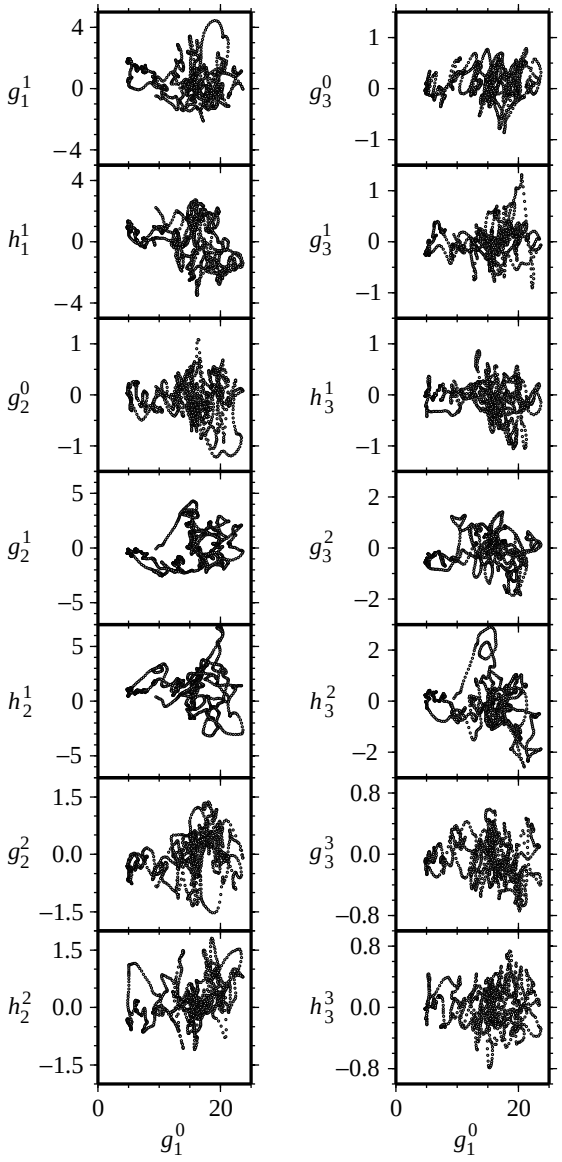

Figure 8. Correlation diagrams between the axial dipole term g_1^0 and the other dipole, quadrupole and octupole terms. Data used are the same as in figure 7.

Figure 8 shows the correlation between the axial dipole and other harmonics up to degree 3. We constructed such diagrams for all of the low-degree Gauss coefficients, but we show only one more (for g_2^2) as an example of correlations between the non-dipole harmonics (figure 9). As shown by the almost circular distribution in each of the parts of figure 9, it can be concluded that there is no correlation between g_2^2 and the other coefficients. The same is true for other non-dipole terms. When treating the long-term statistics of Gauss coefficients, it therefore seems reasonable to assume that they are independent random variables.

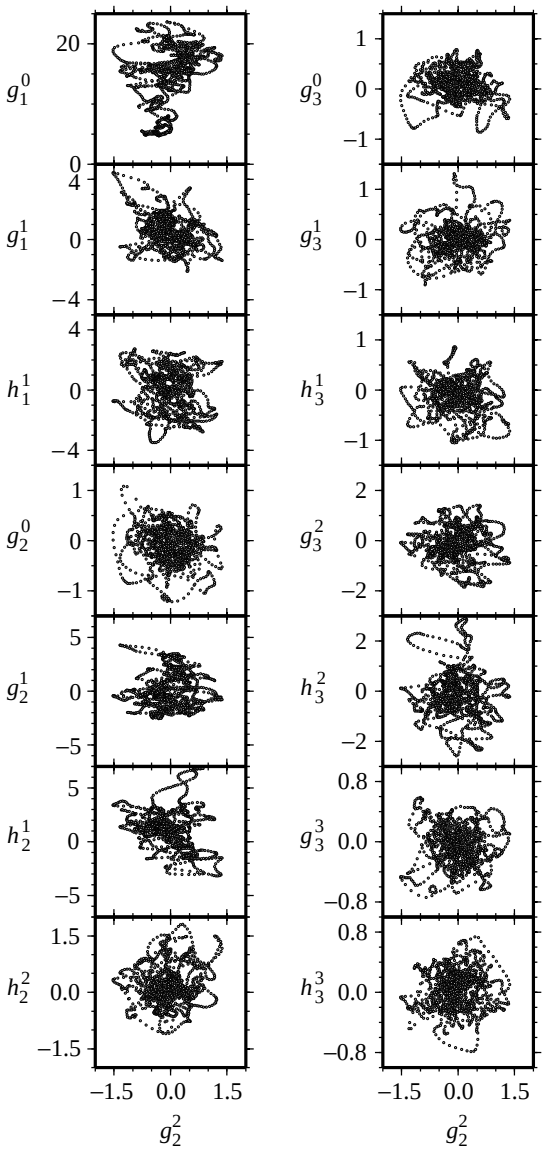

Figure 9. Correlation diagrams between a non-dipole term g_2^2 and the other dipole, quadrupole and octupole terms. Data used are the same as in figure 7.

In the case of g_1^0 (figure 8), it is difficult to decide if it has correlation with other coefficients. There was a short period in the analysed time-interval that the dipole field was particularly weak and stayed in that state for some time (near 3.5 in figure 2). The portions of the scatter diagrams for $g_1^0 < 10$ represent the data from that interval. Figure 8 shows that some correlation might have existed between g_1^0 and other coefficients in that period, as all other coefficients also seem to take smaller values (h_2^2 is no exception, as its magnitude is small compared with g_2^1 or h_2^1). It may be that when the magnetic activity is small, it results in a smaller dipole as well as

smaller fluctuation in non-dipole terms. As this occurred only once in the simulation, it is perhaps premature to draw definite conclusions based on this observation.

4. Discussion

The analysed interval corresponds to about 3×10^4 years. This is much longer than the period of time in which detailed models of the geomagnetic field is available. However, it may still be too short for complete coverage of statistical characteristics of the dynamo process. For example, directional data obtained by palaeomagnetism of lava flows are usually averaged for an interval of 10^5 years or more, in order to obtain the true mean field directions. Thus, interpretation of the present results needs to be carried out with some reservation. Nevertheless, comparison with the observed and conjectured nature of the geomagnetic field results in many interesting findings.

There are a surprisingly large number of characteristics that seem to be shared by both the present and palaeomagnetic fields and the dynamo model. The most important is undoubtedly the dominating role of the dipole, and especially its axial component g_1^0. This may be a basic feature of an Earth-type dynamo.

The statistical properties of Gauss coefficients obtained by the dynamo model seem to be broadly compatible with the assumptions made for modelling palaeosecular variation by Constable & Parker (1988) or by Kono & Tanaka (1995). Excluding the axial dipole term, they seem to behave as zero mean random variables, and their distributions can be well approximated by that of a normal variate. The power of the magnetic field in each degree (except $l = 1$) seems to be about equal at the CMB. At the surface, it shows an exponential decay with degree.

There are differences between the behaviours of the dynamo and the real geomagnetic field. One of the marked differences between the dynamo model and palaeomagnetic field is that the axial quadrupole g_2^0 in the dynamo model does not have a mean significantly different from zero. The existence of persistent g_2^0 is called the dipole offset (Wilson 1970) and seems to be a common feature found in the treatments of palaeomagnetic directional data for the last few million years (e.g. Johnson & Constable 1995). This discrepancy can be attributed to the difference in the boundary conditions at the CMB, or to the shortness of the period covered by the present dynamo simulation. However, it may also be pointed out that palaeointensity data for the same period do not show non-zero g_2^0 terms (Kono *et al.* 2000). In any case, some care is needed for this kind of comparison to be meaningful, similar to the case of westward drift observed at the surface.

5. Summary

The dynamo simulation is, admittedly, still far from representing the real situation in the Earth. Obviously, the approach taken in this study will become more powerful when careful intercomparisons are made between multiple different models, and the working mechanism of the dynamos are more fully understood. Meanwhile, this work presents only a small step in the comparison of simulation results and observed behaviours of the magnetic field. One should be aware of these limitations in discussing the results of this paper.

By analysing the dynamo simulation results, we find a number of points in which these results are quite similar to the observed or conjectured properties of the present and past geomagnetic field. They include the following observations.

(1) The field is dominated by the dipole, especially its axial component g_1^0.

(2) The powers of the magnetic field in each degree of the harmonics measured at the surface decays exponentially. This spectrum becomes nearly flat at the CMB depth (or slightly below). The dipole power is several times larger than the value expected from the trend of nonlinear terms up to about degree 14.

(3) Gauss coefficients, except g_1^0, can be reasonably modelled by random variates with zero mean and variances decreasing with the degree of the harmonic.

(4) The (2,1) Gauss coefficients have much larger variances than other degree-2 coefficients, which agrees with the conclusion reached by statistical treatments of the palaeomagnetic data of the last 5 Myr (e.g. Kono & Tanaka 1995).

There are some properties that are dissimilar between the observed field and the dynamo:

(1) the magnetic fluxes are much more concentrated in small regions at the CMB in the dynamo model;

(2) some of these flux concentrations migrate westward, but there are also areas which migrate eastward; and

(3) the axial quadrupole g_2^0 does not have non-zero mean value.

Some of the differences may point to the need for special consideration of the shortness of the period covered by the dynamo results. Others may be mainly due to the difference between the truncation level of the model description.

Despite the reservations stated above, the present study shows that comparison of dynamo simulation results with the observed (present or palaeomagnetic) data gives instructive results for considering the important properties of the Earth's magnetic field.

We thank David Gubbins and an anonymous reviewer for helpful comments on an earlier manuscript, and Takao Eguchi for assistance in carrying out the computation. The numerical simulation of dynamo models was done on a Cray T3E computer at the National Research Institute for Earth Science and Disaster Prevention under a special project, 'Computational Science', of the Science and Technology Agency. The work of M.K. was partly supported by a research grant (10440124) from Monbusho.

References

Bloxham, J. & Gubbins, D. 1985 The secular variation of Earth's magnetic field. *Nature* **317**, 777–781.

Bloxham, J. & Jackson, A. 1992 Time-dependent mapping of the magnetic field at the core–mantle boundary. *J. Geophys. Res.* **97**, 19 537–19 563.

Bullard, E. C., Freedman, C., Gellman, H. & Nixon, J. 1950 The westward drift of the Earth's magnetic field. *Phil. Trans. R. Soc. Lond.* A **243**, 67–92.

Busse, F. H. 1975 A model of the geodynamo. *Geophys. J. R. Astr. Soc.* **42**, 437–459.

Constable, C. G. & Parker, R. L. 1988 Statistics of the geomagnetic secular variation for the past 5 m.y. *J. Geophys. Res.* **93**, 11 569–11 581.

Glatzmaier, G. A. 1984 Numerical simulation of stellar convective dynamos. I. The model and method. *J. Comp. Phys.* **55**, 461–484.

Glatzmaier, G. A. & Roberts, P. H. 1995*a* A three-dimensional convective dynamo solution with rotating and finitely conductive inner core and mantle. *Phys. Earth Planet. Interiors* **91**, 63–75.

Glatzmaier, G. A. & Roberts, P. H. 1995*b* A three-dimensional self-consistent computer simulation of a geomagnetic field reversal. *Nature* **377**, 203–209.

Gubbins, D. & Bloxham, J. 1985 Geomagnetic field analysis. III. Magnetic fields on the core–mantle boundary. *Geophys. J. R. Astr. Soc.* **80**, 695–713.

Gubbins, D. & Kelly, P. 1995 On the analysis of paleomagnetic secular variation. *J. Geophys. Res.* **100**, 14 955–14 964.

Gubbins, D. & Roberts, P. H. 1987 Magnetohydrodynamics of the Earth's core. In *Geomagnetism* (ed. J. A. Jacobs), vol. 2, pp. 1–183. Academic.

Johnson, C. & Constable, C. G. 1995 The time averaged field as recorded by lava flows over the past 5 Myr. *Geophys. J. Int.* **122**, 489–519.

Kageyama, A. & Sato, T. 1995 Computer simulation of a magnetohydrodynamic dynamo. II. *Phys. Plasmas* **2**, 1421–1431.

Kono, M. & Tanaka, H. 1995 Mapping the Gauss coefficients to the pole and the models of paleosecular variation. *J. Geomag. Geoelectr.* **47**, 115–130.

Kono, M., Tanaka, H. & Tsunakawa, H. 2000 Spherical harmonic inversion of paleomagnetic data: the case of linear mapping. *J. Geophys. Res.* **105**, 5817–5833.

Langel, R. A. 1987 The main field. In *Geomagnetism* (ed. J. A. Jacobs), vol. 1, pp. 249–512. Academic.

Langel, R. A. & Estes, R. H. 1982 A geomagnetic field spectrum. *Geophys. Res. Lett.* **9**, 250–253.

Langel, R. A., Estes, R. H., Mead, G. D., Fabiano, E. B. & Lancaster, E. R. 1980 Initial geomagnetic field model from magsat vector data. *Geophys. Res. Lett.* **7**, 793–796.

Lowes, F. J. 1974 Spatial power spectrum of the main geomagnetic field, and extrapolation to the core. *Geophys. J. R. Astr. Soc.* **36**, 717–730.

Sakuraba, A. & Kono, M. 1999 Effect of the inner core on the numerical solution of the magnetohydrodynamic dynamo. *Phys. Earth Planet. Interiors* **111**, 105–121.

Wilson, R. L. 1970 Permanent aspects of the Earth's non-dipole magnetic field over upper tertiary times. *Geophys. J. R. Astr. Soc.* **19**, 417–437.

Yukutake, T. 1967 The westward drift of the Earth's magnetic field in historic times. *J. Geomag. Geoelectr.* **19**, 103–116.

Yukutake, T. & Tachinaka, H. 1968 The nondipole part of the Earth's magnetic field. *Bull. Earthquake Res. Inst. Univ. Tokyo* **46**, 1027–1074.

PHILOSOPHICAL TRANSACTIONS OF THE ROYAL SOCIETY A MATHEMATICAL, PHYSICAL & ENGINEERING SCIENCES